CHIN. PHYS. LETT. Vol. 35, No. 6 (2018) 066101

Self-Similar Transformation and Vertex Configurations of the Octagonal Ammann–Beenker Tiling *

Hong-Mei Zhang(张红梅), Cheng Cai(蔡程), Xiu-Jun Fu(傅秀军)**

School of Physics and Optoelectronics, South China University of Technology, Guangzhou 510640

(Received 27 December 2017)

Based on the matching rules for squares and rhombuses, we study the self-similar transformation and the vertex configurations of the Ammann–Beenker tiling. The structural properties of the configurations and their relations during the self-similar transformation are obtained. Our results reveal the distribution correlations of the configurations, which provide an intuitive understanding of the octagonal quasi-periodic structure and also give implications for growing perfect quasi-periodic tiling according to the local rules.

PACS: *61.44.Br*, *61.50.Ah*, *02.60.Cb* DOI: 10.1088/0256-307X/35/6/066101

Quasicrystals may possess five-fold or more than six-fold rotational symmetries which are forbidden in traditional periodic crystals.[1–3] As an eight-fold symmetrical structure, the Ammann–Beenker tiling (ABT)[4,5] plays an important role in theoretical models for quasicrystals. The ABT is an aperiodic tiling composed of squares and rhombuses, which can be generated either by an aperiodic set of prototiles or by the cut-and-project method. The ABT has some properties that are similar to the famous Penrose tiling, including the quasi-periodic translational order, the self-similarity, and the matching rules. The diffraction pattern of the ABT structure reveals both the eight-fold symmetry and the long-range order.

The self-similar property and the quasi-periodic tiling way for squares and rhombuses have been studied by Ammann *et al.*[4] and Beenker,[5] respectively, which are fundamental issues for a quasilattice. Based on the ABT model, some physical properties have been studied and novel results in many fields have been revealed, such as the phason defect in simple octagonal quasicrystals,[6] critical eigenstates and multifractal spectra for a class of tight-binding Hamiltonians,[7] Fano-type guided resonances in aperiodically-ordered photonic quasicrystal slabs,[8] as well as the high-temperature expansions[9] and the Lee–Yang zeros for the Ising model in quasi-periodic tilings.[10]

Even though the matching rules[11] and the self-similar transformation[12] of the ABT were proposed after the experimental discovery of quasicrystals,[13] the structural properties have not been extensively studied compared with the well-known Penrose tiling. It is generally believed that, under certain conditions, atoms may aggregate into a quasi-periodic solid rather than a periodic one. However, a quasilattice is much more complicated than a periodic one, and the growth mechanisms of a perfect quasicrystal have not been thoroughly understood. Prototiles plus matching rules may provide a reasonable way to explain the formation of a quasicrystal, such as the edge-to-edge matching for fat and skinny rhombi in a Penrose tiling. However, mismatch in the process of tiling will occur inevitably because the matching rules only constrain the local order. Regarding this shortcoming, a growth algorithm based on the vertex rules was developed by Onoda *et al.*[14] The fact that only eight vertex configurations are allowed in a perfect Penrose tiling requires that adding a tile to the boundary of the existed pattern must not produce new configurations beyond the eight ones. If there is only one choice to add a rhombus, the growth will guarantee the correct tiling and the procedure can go a further step. If, however, there is more than one way to add a rhombus, proper strategies should be taken into account.

In this Letter, we focus on the eight-fold symmetric ABT and investigate its geometric properties during the self-similar transformation and the tiling process. An ideal ABT can be produced by the self-similar transformation starting from a square or a rhombus of 45° acute angle as the prototypes, as shown in Fig. 1. A square is divided into nine parts consisting of one small square, four rhombuses and four halves of square as shown in Fig. 1(a). A half small square will combine the adjacent half one resulting from the transformation outside the original large square and thus will form a full square. Based on this analysis, we obtain that a square will produce three smaller squares and four smaller rhombuses after one transformation. Similarly, a rhombus will produce two smaller squares and three smaller rhombuses after one transformation as shown in Fig. 1(b). After three such transformations, we obtain the fourth generation of the patterns as shown in Figs. 1(c) and 1(d).

*Supported by the National Natural Science Foundation of China under Grant No 11674102.

**Corresponding author. Email: phxjfu@scut.edu.cn

© 2018 Chinese Physical Society and IOP Publishing Ltd

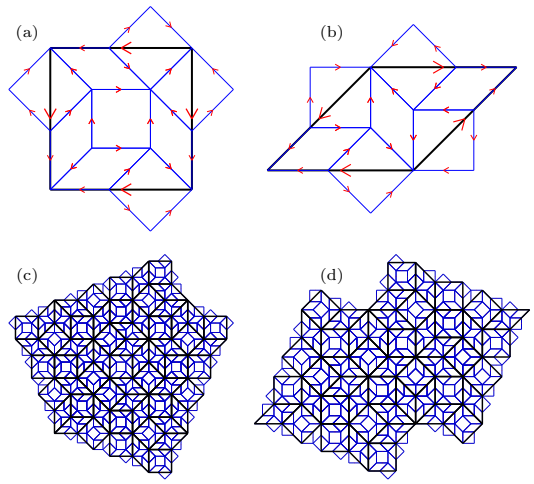

Fig. 1. The self-similar transformation for (a) the square and (b) the rhombus with acute angle of 45°. [(c), (d)] The ABT patterns after three self-similar transformations starting from a square and a rhombus, respectively. The thick and thin lines represent the third generation and the fourth generation of the patterns in (c) and (d), respectively.

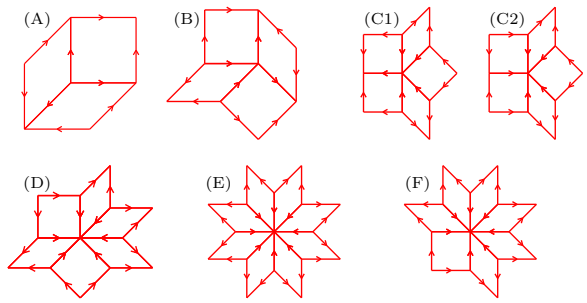

Fig. 2. Seven types of vertex in the Ammann–Beenker tiling.

Let x be the ratio of the number of squares to the total number of tiles and y be the ratio of the number of rhombuses to the total number of tiles, then the ratios before and after the transformation keep unchanged for an infinitely large patterns. Hence we have

$$\frac{3x+2y}{(3x+2y)+(4x+3y)}=x,$$
$$\frac{4x+3y}{(3x+2y)+(4x+3y)}=y.$$

Solving these equations, we obtain irrational solutions $x=\sqrt{2}-1$ and $y=2-\sqrt{2}$. Analogous to the golden mean $\tau=(\sqrt{5}-1)/2$ widely used in quasicrystals, the solution for x is called the silver mean and is denoted as σ.[15]

The vertex configurations in a quasi-periodic pattern are characteristics of the structure which confine the arrangement of adjacent tiles. Even though they are local rules, the effect spreads out to a large scale in the tiling process. In a Penrose tiling, there are eight types of vertex configurations, which have been employed to generate perfect quasi-periodic patterns.[16] In the ABT, if we combine the squares and rhombuses in a way so that the sum of the angles at the vertex is 360° and the arrows on the edges match one another, there will be 19 types. However, some of them never appear in an ideal ABT, such as the configuration composed of four squares. Therefore, we identify the vertex configuration from a large pattern generated by the self-similar transformation, and seven types of vertices are found, which are named as A–F shown in Fig. 2. Note that types C1 and C2 are composed of the same prototiles but the difference is that the arrow of the common side of two squares is outward for C1 but inward for C2.

To find the ratio of the number of one kind of vertex to the total number of vertices, we analyze the self-similar transformation. During this process, more tiles evolve, and they share sides and vertices, which seems difficult to obtain the relationships between the number of vertices before and after the transformation. We will adopt the following rules to compute the number of vertices. Considering one original vertex as the center, after one transformation, if a new vertex is located inside the tile and shared by N vertices, then the contribution of the original vertex is set to be $1/N$. On the other hand, if the new vertex lies on a side and is shared by two vertices, then the contribution of the original vertex is $1/2$. Taking type A as an example, after one transformation, the original vertex A is replaced by the new vertex C2. At the edges of the configuration of C2, three A, six B and one C1 are presented. Three A are shared by two original vertices respectively because they locate on the three sides. Since two B lie on the position of vertex of original configuration, they should not be taken into consideration. The rests of B and C1 are shared by three original vertices separately judging by the distance of the nearest neighbor. Therefore, one type A vertex will become C2+(3/2)A+(4/3)B+(1/3)C1. All the transformations for the seven types of vertex configurations are listed as follows:

$$\begin{aligned}
\mathrm{A} &\to \mathrm{C2}+(3/2)\mathrm{A}+(4/3)\mathrm{B}+(1/3)\mathrm{C1},\\
\mathrm{B} &\to \mathrm{D}+2\mathrm{A}+2\mathrm{B}+(2/3)\mathrm{C1},\\
\mathrm{C1} &\to \mathrm{F}+(7/2)\mathrm{A}+(8/3)\mathrm{B}+(2/3)\mathrm{C1},\\
\mathrm{C2} &\to \mathrm{E}+(11/2)\mathrm{A}+(11/3)\mathrm{B},\\
\mathrm{D} &\to \mathrm{E}+5\mathrm{A}+(10/3)\mathrm{B},\\
\mathrm{E} &\to \mathrm{E}+4\mathrm{A}+(8/3)\mathrm{B},\\
\mathrm{F} &\to \mathrm{E}+(9/2)\mathrm{A}+3\mathrm{B}.
\end{aligned}$$

Suppose that the numbers of the seven types of vertex configurations before transformation are N_{A}, N_{B}, N_{C1}, N_{C2}, N_{D}, N_{E} and N_{F}, respectively, and these numbers become N'_{A}, N'_{B}, N'_{C1}, N'_{C2}, N'_{D}, N'_{E} and N'_{F}, respectively, after the transformation,

then from the above analysis we have

$$
\begin{aligned}
N'_{\rm A} &= (3/2)N_{\rm A} + 2N_{\rm B} + (7/2)N_{\rm C1} + (11/2)N_{\rm C2} \\
&\quad + 5N_{\rm D} + 4N_{\rm E} + (9/2)N_{\rm F}, \\
N'_{\rm B} &= (4/3)N_{\rm A} + 2N_{\rm B} + (8/3)N_{\rm C1} + (11/3)N_{\rm C2} \\
&\quad + (10/3)N_{\rm D} + (8/3)N_{\rm E} + 3N_{\rm F}, \\
N'_{\rm C1} &= (1/3)N_{\rm A} + (2/3)N_{\rm B} + (2/3)N_{\rm C1}, \\
N'_{\rm C2} &= N_{\rm A}, \\
N'_{\rm D} &= N_{\rm B}, \\
N'_{\rm E} &= N_{\rm C2} + N_{\rm D} + N_{\rm E} + N_{\rm F}, \\
N'_{\rm F} &= N_{\rm C1}.
\end{aligned}
$$

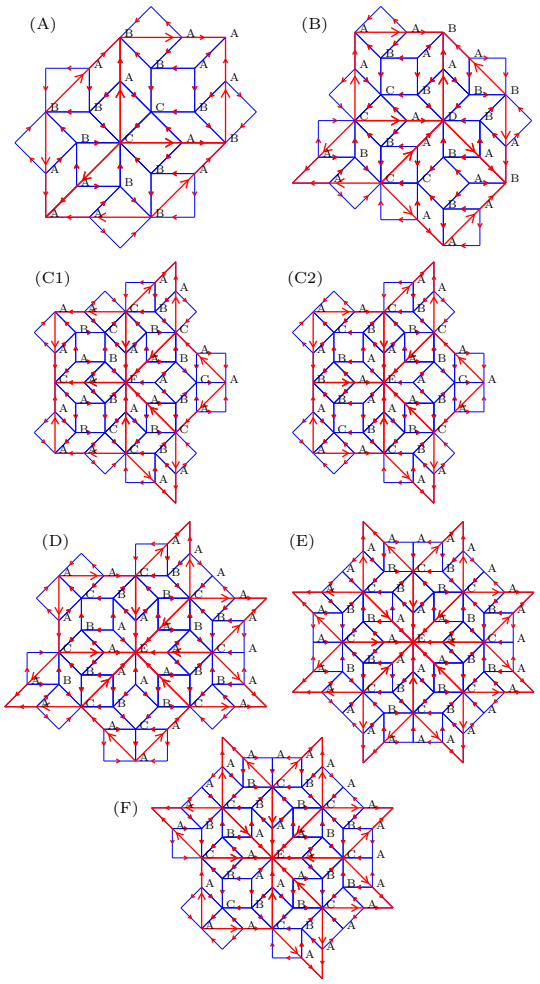

Fig. 3. The vertex evolution after a self-similar transformation.

After the self-similar transformation, the total numbers of the vertices increase by a factor $k = (25/6)a + (17/3)b + (47/6)c_1 + (61/6)c_2 + (28/3)d + (23/3)e + (17/2)f$. For an infinitely large quasi-periodic ABT, the ratios of the seven types of configurations keep unchanged after a self-similar transformation. Therefore, if we denote the ratios of the seven vertices by a, b, c_1, c_2, d, e and f, respectively, then we have

$$
\begin{aligned}
&((3/2)a + 2b + (7/2)c_1 + (11/2)c_2 + 5d \\
&+ 4e + (9/2)f)/k = a, \\
&((4/3)a + 2b + (8/3)c_1 + (11/3)c_2 + (10/3)d \\
&+ (8/3)e + 3f)/k = b, \\
&((1/3)a + (2/3)b + (2/3)c_1)/k = c_1, \\
&a/k = c_2, \\
&b/k = d, \\
&(c_2 + d + e + f)/k = e, \\
&c_1/k = f.
\end{aligned}
$$

The solutions are obtained by the use of Mathmatica,

$$
\begin{aligned}
&a = 0.4142136,\ b = 0.3431458,\ c_1 = 0.07106781, \\
&c_2 = 0.07106781,\ d = 0.05887450,\ e = 0.02943725, \\
&f = 0.01219331.
\end{aligned}
$$

To obtain the analytical expressions for the above results, we use the silver mean $\sigma = \sqrt{2} - 1$ to fit the seven ratios. The main idea is that, in a quasi-periodic structure, many geometric parameters can be expressed in term of polynomial expansion of the silver mean. The fitted results are

$$
\begin{aligned}
&a = \sigma,\ b = 2\sigma^2,\ c_1 = \sigma^3,\ c_2 = \sigma^3, \\
&d = 2\sigma^4,\ e = \sigma^4,\ f = \sigma^5.
\end{aligned}
$$

The normalization is confirmed by observing that $\sigma + 2\sigma^2 + 2\sigma^3 + 3\sigma^4 + \sigma^5 = 1$.

To double check the above results, we generate large patches of the ABT by a self-similar transformation method starting from several different clusters and carry out statistics on the number of vertex configurations. Table 1 lists the ratios of the numbers of seven configurations to the total number of vertices consisting of 7980 vertices generated from a square after five self-similar transformations. The numerical results match the analytical ones within four significant figures, where the errors are due to the finite number of tiles.

Table 1. Numerical results of the numbers of and ratios of the seven types of configurations. The ABT consists of 7980 vertices generated by self-similar transformation starting with a square.

Type	Number	Ratio
A	3305	0.4142
B	2786	0.3491
C1	553	0.0693
C2	553	0.0693
D	478	0.0599
E	216	0.0271
F	89	0.0112

Although some results about configurations of the Penrose tiling have been discussed,[17] here we give

comparisons with those of the ABT. It is obvious that the decorations of the ABT look much more complicated than those for the Penrose tiling.[6] For the process of the self-similar transformation, the growth rate of the tiles of the ABT is much faster than that of the Penrose tiling. This means that if we intend to obtain the ABT patterns which are of the same generation as the Penrose tiling after several self-similar transformations, more tiles and vertices would be obtained and processed. Furthermore, the E configuration with eight-fold symmetry does not appear as often in the ABT as the configuration with five-fold symmetry in the Penrose tiling.

Attention should also be paid to the vertex configurations. Unlike the classification approach proposed by de Bruijn[18] and the requirement for continuity of the Ammann lines[14] to obtain the eight vertex types in the Penrose tiling, we obtain vertex types straightforward through geometrical analysis on a large pattern of the ABT generated by the self-similar transformation. When analyzing the relationship of vertices before and after the transformation, we adopt rules that are different from those used in the Penrose tiling. Studying the vertex evolution after a self-similar transformation, we find that the contribution of the original vertex making the new one cannot be simply identified by the position of the new vertex. For example, if a new vertex is located inside the tile, it is not simply shared by four original vertices. Rather, we should consider whether the new vertex belongs to the points of the vertex configuration of original vertices but not its location. In addition, it is the original center vertex and the points of the vertex configuration of the new center vertex that should be taken into account instead of all new vertices in tiles of the original vertex configuration.

In summary, we have used the self-similar transformation method to generate the ABT. The vertex configurations of the ABT, the structural properties of the configurations and their relations during the self-similar transformation are presented. The ratios of vertex configurations are expressed in term of polynomial expression of the silver mean in the ABT similar to the usage of the golden mean in the Penrose tiling, but indicating different quasi-periodic arrangements and orders. The vertex configuration types and the evolution during the self-similar transformation can be used to study rules for growing perfect quasi-periodic patterns.

References

[1] Shechtman D, Blech I, Gratias D et al 1984 *Phys. Rev. Lett.* **53** 1951
[2] Levine D and Steinhardt P J 1984 *Phys. Rev. Lett.* **53** 2477
[3] Liu Y Y and Fu X J 1999 *Quasicrystals* (Shanghai: Shanghai Scientific and Technological Education Publishing House) (in Chinese)
[4] Ammann R, Grünbaum B and Shephard G C 1992 *Discrete Comput. Geom.* **8** 1
[5] Beenker F P M 1982 *Algebraic Theory Non-periodic Tilings By Two Simple Building Blocks: A Square A Rhombus* (Eindhoven Tech. University: TH-Report 82-WSK-04)
[6] Socolar J E S 1989 *Phys. Rev.* B **39** 10519
[7] Macé N, Jagannathan A, Kalugin P et al 2017 *Phys. Rev.* B **96** 045138
[8] Ricciardi A, Pisco M, Cutolo A et al 2011 *Phys. Rev.* B **84** 085135
[9] Repetowicz P, Grimm U and Schreiber M 1999 *J. Phys.* A **32** 4397
[10] Simon H and Baake M 1997 *J. Phys.* A **30** 5319
[11] Jaric M V 1989 *Introduction to the Mathematics of Quasicrystals, Aperiodicity and Order* (San Diego: Academic Press)
[12] Goodman-Strauss C 1998 *Ann. Math.* **147** 181
[13] Wang N, Chen H and Kuo K H 1987 *Phys. Rev. Lett.* **59** 1010
[14] Onoda G Y, Steinhardt P J, Divincenzo D P et al 1988 *Phys. Rev. Lett.* **60** 2653
[15] Gumbs G and Ali M K 1988 *Phys. Rev. Lett.* **60** 1081
[16] Jeong C H 2007 *Phys. Rev. Lett.* **98** 135501
[17] Peng B Y and Fu X J 2015 *Chin. Phys. Lett.* **32** 056101
[18] de Bruijn N G 1981 *Ned. Akad. Wetensch. Prosc. Ser.* A **43** 39